Electronic supporting information

for

Framework structured $Na_4Mn_4Ti_5O_{18}$ as electrode for Na-ion storage hybrid devices

M. Jayakumar[a‡], K. Hemalatha[a,b‡], K. Ramesha[a,b] and A. S. Prakash[a,b]*

[a]CSIR Central Electrochemical Research Institute-Chennai Centre,CSIR-Madras Complex, Taramani, Chennai-600 113, India.CSIR−Network Institutes of Solar Energy (CSIR−NISE)

[b]Academy of Scientific and Innovative Research (AcSIR), CSIR Central Electrochemical Research Institute-Chennai Centre, CSIR-Madras Complex, Taramani, Chennai-600 113, India

* Corresponding author
‡ These authors contributed equally to this work

The unit convention used in this article is as follows.

The relation between capacity in mAh and coloumbs is according to the equation

1 mAh = 3.6 C

Relation between capacity and specific capacity is

Specific capacity (in F) = capacity (in C) / Potential window (in V)

The specific discharge capacity Q (F/g) is calculated according to the following equation^

$Q = I\Delta t/m\Delta V$

where I is the applied working current, Δt represents the discharge time, ΔV (V) is the voltage range, and m (g) is the mass of active materials.

Specific capacity can also be expressed in mAh/g, which is directly calculated according to the following equation

$Q = I\Delta t/m$

^ B.H. Zhang, Y. Liu, Z. Chang, Y.Q. Yang, Z.B. Wen, Y.P. Wu, R. Holze, *J. Power Sources* 253 (2014) 98-103

Supporting information S1

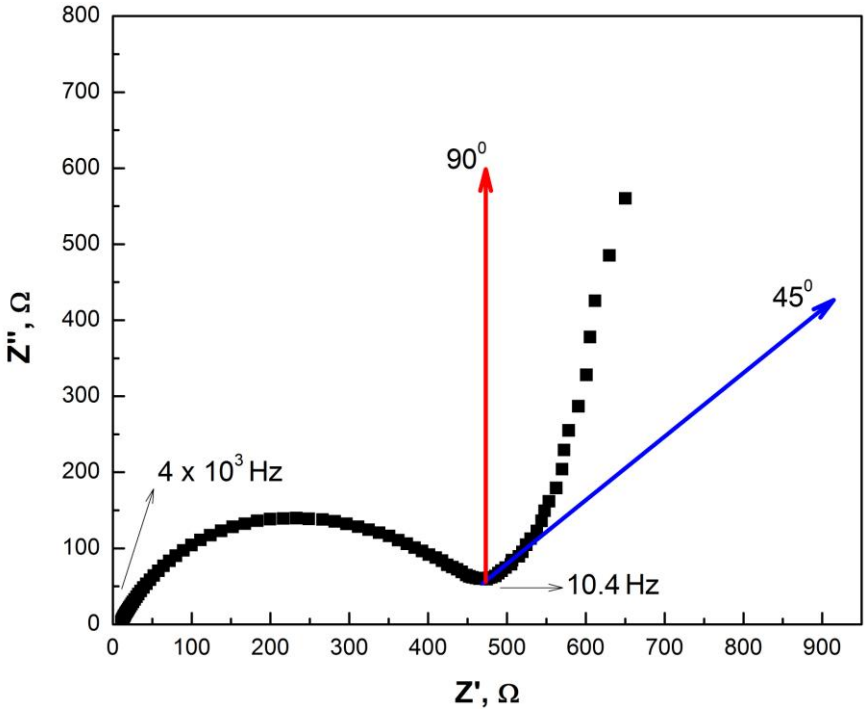

Electrochemical Impedance Spectroscopy (EIS) analysis to ascertain the charge storage mechanism in $Na_4Mn_4Ti_5O_{18}$.

The sample was charged up to 3.95 V (Vs. Na^0/Na^+). Then, EIS measurement was performed at this potential (3.95 V vs. Na^0/Na^+) in the frequency range 4 x 10^3 Hz – 5 x 10^{-3} Hz. The resultant Nyquist plot (Z″ vs. Z′) is presented above. The Nyquist plot typically consists of a high frequency semicircle and a low frequency spike. Typically, the high frequency semicircle is associated with, the internal resistance of electrode, interface resistance and charge transfer resistance. In the low frequency region, typical linear shape of Nyquist plot can be observed where the slope gradually changes from 45° to 90° with decrease of ac frequency, indicating that the Na-intercalation in $Na_4Mn_4Ti_5O_{18}$ is not only controlled by the diffusion process.[23] In other words, this result clearly demonstrates that $Na_4Mn_4Ti_5O_{18}$ intercalates Na^+ through pseudocapacitive processes.

Supporting information S2

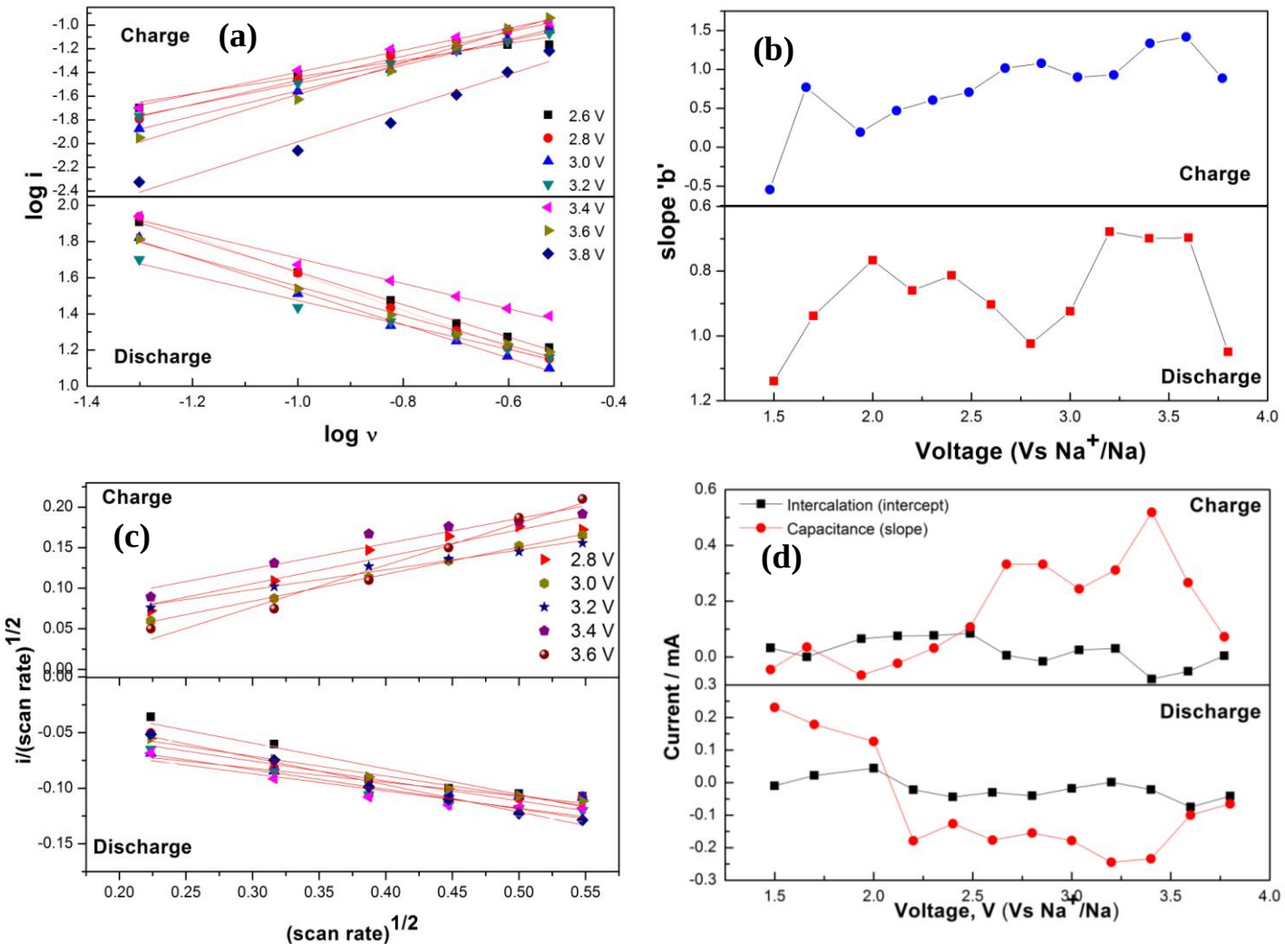

Electrochemical analysis of charge storage in $Na_4Mn_4Ti_5O_{18}$ using cyclic voltammetry. (a) Plot of log i versus log scan rate at different voltages, (b) Slope 'b' obtained from linear plot of log I vs log scan rate at different voltages, (c) Plot of i/(scan rate)$^{1/2}$ versus (scan rate)$^{1/2}$ and (d) contribution from intercalation and capacitance towards total current in cyclic voltammogram at different voltages.

Cyclic voltammograms of $Na_4Mn_4Ti_5O_{18}$ was recorded at different scan rates. Fig. S2(a) shows linear relationship between log current versus log scan rate and slope indicates the charge storage mechanism in $Na_4Mn_4Ti_5O_{18}$ involves capacitance in addition to intercalation (Fig. S2(b)[10,11,24]. In the plot of i/(scan rate)$^{1/2}$ versus (scan rate)$^{1/2}$ (shown in Fig. S2(c)) the intercept

corresponds to contribution of intercalation and slope corresponds to the capacitance contribution towards total current. As observed in Fig. S2(d), the current contribution from capacitance dominates intercalation in most voltages. The analysis indicates that $Na_4Mn_4Ti_5O_{18}$ stores electrochemical energy via both intercalation and capacitive modes.

Supporting information S3

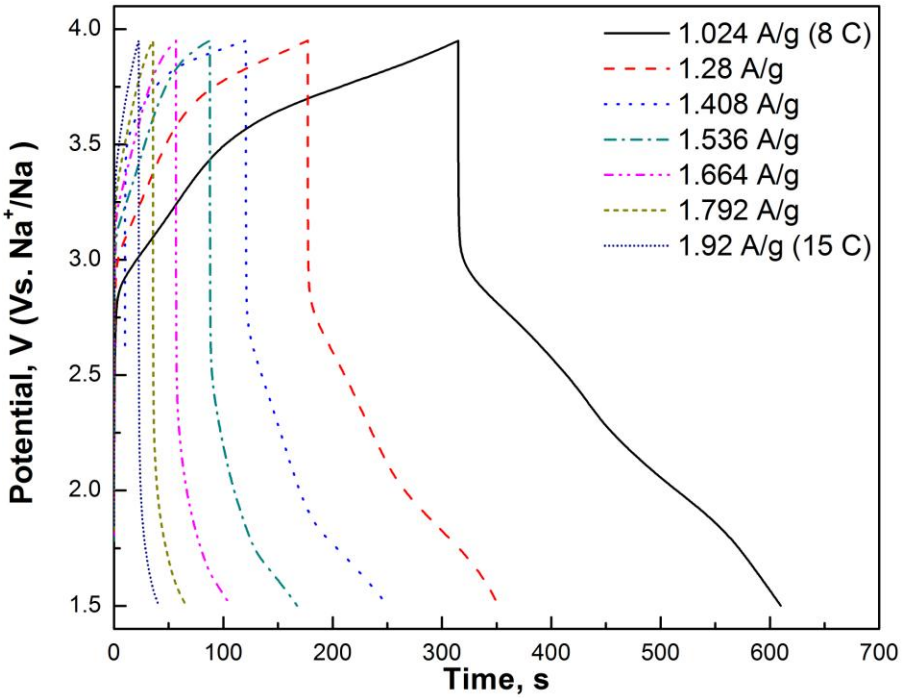

Performance of $Na_4Mn_4Ti_5O_{18}$ hybrid electrode at fast cycling rates. Potential vs time plot at different rates for $Na_4Mn_4Ti_5O_{18}$ Vs. Na cell in 1M $NaPF_6$/EC-DMC organic electrolyte.

The charge-discharge plot of $Na_4Mn_4Ti_5O_{18}$ in organic electrolyte clearly exhibits hybrid performance. An ideal capacitor exhibits triangular galvanostatic charge – discharge behavior with no voltage drop. Since the charge-storage mechanism in $Na_4Mn_4Ti_5O_{18}$ involves intercalation as well as capacitance, the charge – discharge profile is not triangular. Besides a voltage drop of about 1.0 V observed during discharging from 3.95 V, the non-linear region between 3 V and 1.5 V clearly exhibits multiple charge storage mechanisms – intercalation and pseudocapacitance.

Supporting information S4

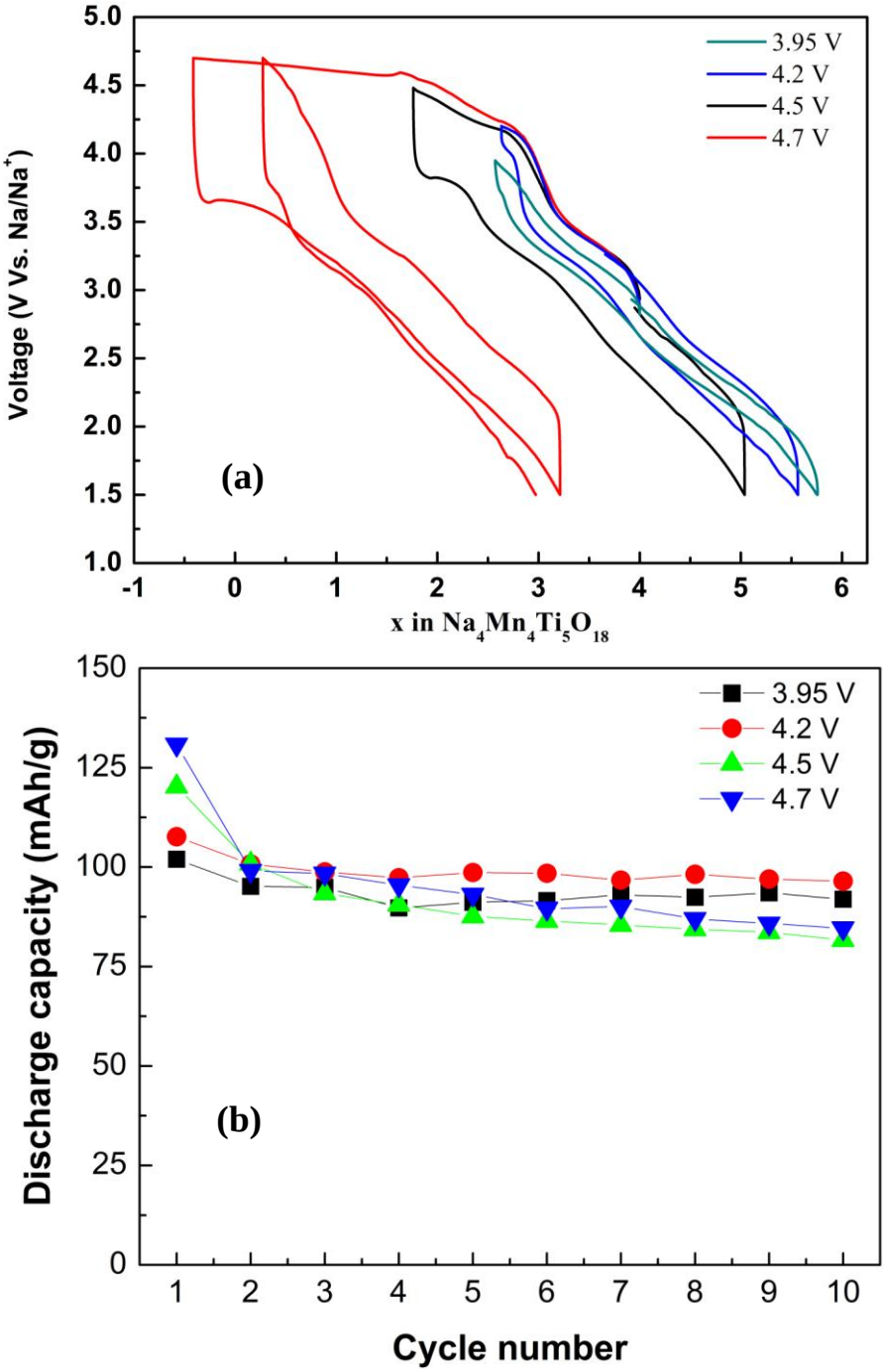

Electrochemical performance of $Na_4Mn_4Ti_5O_{18}$ as cathode material subjected to galvanostatic charge-discharge at various cathodic cutoff potentials at C/10 rate. The lower potential was fixed at 1.5 V (Vs Na) in all experiments. Electrolyte : 1M $NaPF_6$ in EC-DMC (a) Voltage – composition plot of $Na_4Mn_4Ti_5O_{18}$ rate at different cathodic cut-off potentials. (b) Capacity retention plots derived from cycling at various cathodic potentials.

Galvanostatic charge discharge data for different cathodic voltages at C/10 rate are shown in Fig. S4(a) and respective discharge capacity versus cycle number are compared in Fig. S4(b). When charged up to 4.5 V, nearly 2 Na is removed whereas almost all the 4 Na ions are removed when the potential limit was 4.7 V due to the large plateau between 4.5 and 4.7 V (Fig. S4(a)). The corresponding first discharge capacity for the 4.7 V cycling is 128 mAh/g (Fig. S4(b)). This irreversible loss can arise due to two reasons; either irreversible degradation of the active material and/or the electrolyte[25]. Although first cycle irreversibility was observed at all cathodic potentials, it was limited to 6-7% when cycled at potentials ≤4.2 V. Also the respective capacity retention was fairly high (Fig. S4(b)). After 10 cycles, capacity retention values were 91%, 88%, 68% and 64% when the reversal cathodic potential were 3.95 V, 4.2 V, 4.5 V, 4.7 V, respectively. Although, 4.2 V and 3.95 V data exhibited similar discharge capacity and capacity retention, 3.95 V has least 1st cycle loss and better faradaic efficiency. Therefore, this potential was chosen for long cycling experiments.

Supporting information S5

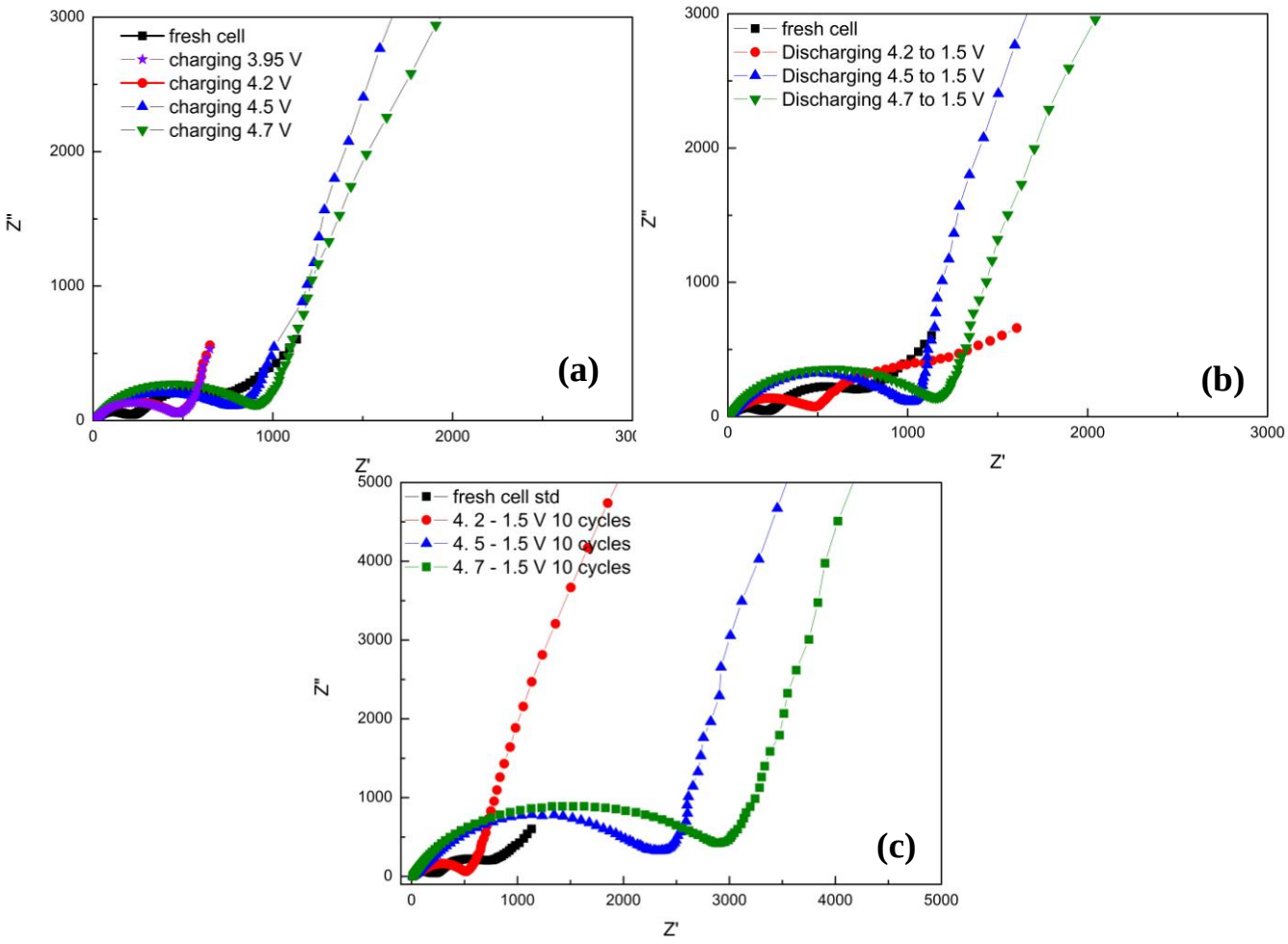

Electrochemical impedance data of $Na_4Mn_4Ti_5O_{18}$ vs Na cells recorded after cycling at different cathodic cut-off potentials at C/10 rate. The lower potential was fixed at 1.5 V (Vs Na) in all experiments. Electrolyte: 1M $NaPF_6$ in EC-DMC (a) After 1st charging (b) After subsequent discharge (c) After 10 cycles

The relation between cathodic voltage limit and discharge capacity as evidenced in S4 was further investigated using electrochemical impedance spectroscopy. Potentiostatic impedance was recorded under three conditions - after charging at different voltages, subsequent discharging to 1.5 V (Vs. Na) and after 10 cycles at respective voltages and the results are presented in S5. As evidenced from Fig. S5(a) there is large resistance across SEI when cycled up to 4.5 V and 4.7 V whereas the values are relatively low for 3.95 V and 4.2 V (~ 430 Ω). Upon completing the first cycle, the trend remained same although there is slight increase in R_{SEI}

values at higher voltages (Fig. S5(b)). However after 10 cycles, the disparity in resistance values becomes very large between cells cycled ≤4.2 V and ≥4.5 V. While the resistance values of 4.2 V remained similar, multifold increase in resistance in cells ≥4.5 V were observed (Fig. S5(c)). The increase in interfacial resistance for voltages > 4.5V is attributed to thick solid electrolyte interface (SEI) as a consequence of electrolyte degradation at high potential.